



Effects of annealing on the tensile properties of irradiated austenitic stainless steel ¹

I. Ioka ^{a,*}, A. Naito ^a, K. Shiba ^a, J.P. Robertson ^b, S. Jitsukawa ^a,
A. Hishinuma ^a

^a Department of Nuclear Energy System, Japan Atomic Energy Research Institute, 2-4 Shirakata, Tokai-mura, Ibaraki-ken 319-1195, Japan

^b Metals and Ceramics Division, Oak Ridge National Laboratory, P.O. Box 2008, Oak Ridge, TN 37831-6376, USA

Abstract

The austenitic stainless steel (Fe–0.06C–0.5Si–1.8Mn–14Cr–16Ni–2Mo–0.24Ti) was irradiated in a triple ion facility and the High Flux Isotope Reactor. The materials used were in the solution annealed (SA) and 15% cold-worked (CW) condition. TEM and tensile specimens were irradiated to a dose level of 30 and 10 dpa at 200°C. Some of the specimens were annealed after the irradiation at 500°C for 8 h in a vacuum. Microhardness tests were carried out on the surface of the TEM disks at room temperature. Tensile tests were carried out at 200°C in a vacuum with strain rate of about $1 \times 10^{-3} \text{ s}^{-1}$. The microhardness of both SA and CW increased by ion irradiation and then decreased by annealing. The yield strengths of the neutron irradiated SA and CW decreased to 610 and 650 MPa by annealing, respectively. The strain to necking of the irradiated CW recovered from 0.7% to 7.6%. The fracture mode remained ductile in each case. © 1998 Elsevier Science B.V. All rights reserved.

1. Introduction

Type 316 austenitic stainless steel has been selected as a candidate material for the first wall and blanket structures of the International Thermonuclear Experimental Reactor (ITER). The anticipated operating temperature and neutron dose for the material are evaluated for temperatures up to 450°C and for neutron doses up to 25 dpa. Much data on 316 stainless steels at the irradiation condition have previously been accumulated [1–4]. Most hardening and degradation of ductility of 316 stainless steel occurs in the temperature range from 250°C to 350°C. The strain hardening capacity of the irradiated material is lower than that of the unirradiated. In particular, the uniform elongation (Eu) de-

creases to less than 0.5% in the vicinity of 300°C after irradiation. The decrease in Eu has raised concerns over using 316 stainless steel in ITER. For Eu greater than 5%, the material is considered to be sufficiently ductile for ASME Code rules to be applicable; for the semi-brittle ($1\% < \text{Eu} \leq 5\%$) and brittle ($\text{Eu} \leq 1\%$) regimes, a different design rule needs to be adopted [5].

Previous observations have indicated that heat treatments have the potential of restoring mechanical properties of irradiated materials. For example, the fine scale black dot damage structure found in irradiated 304 stainless steel disappeared when the specimen was annealed in the range from 400°C to 600°C [6]. Jacobs et al. [7] reported that the hardness of 304 stainless steel irradiated to fast neutron fluences up to $3 \times 10^{21} \text{ n/cm}^2$ ($E > 1 \text{ MeV}$) became lower after annealing at 500°C for 1 h.

To gain insights into the effect of annealing on the tensile properties, the first step is to examine the change in hardness of an ion irradiated material after annealing; the second step is to compare the tensile properties of a neutron irradiated specimen with that of an irradiated one after annealing. It is the purpose of this paper to make clear that the tensile properties of irradiated 316 austenitic stainless steel can be restored by annealing.

* Corresponding author. Tel.: +81 29 282 6385; fax: +81 29 282 6489; e-mail: ioka@popsvr.tokai.jaeri.go.jp.

¹ Research sponsored by Japan Atomic Energy Research Institute and the Office of Fusion Energy, US Department of Energy, under contract DE-AC05-84OR21400 with Lockheed Martin Energy Research.

Table 1
Chemical compositions of the JPCA

| Alloy | Chemical composition (wt%) | | | | | | | | | | | | |
|-------|----------------------------|------|-----|------|-------|-------|------|-------|------|------|-------|-------|-------|
| | Fe | C | Si | Mn | P | S | Ni | Cr | Mo | Ti | B | N | Co |
| JPCA | bal. | 0.06 | 0.5 | 1.77 | 0.027 | 0.005 | 15.6 | 14.22 | 2.28 | 0.24 | 0.003 | 0.004 | 0.002 |

2. Experimental procedure

The materials tested were a Japan Primary Candidate Alloy (JPCA) in the solution-annealed (SA) and 15% cold-worked (CW) condition. The chemical composition of the material is given in Table 1. The JPCA was modified from type 316 stainless steel to improve the swelling properties under neutron irradiation. The specimens were in the form of TEM disks for ion irradiation and in the form of SS-3 flat tensile specimens for neutron irradiation. The TEM disks were 3 mm diameter by 0.2 mm thick. The gauge section of SS-3 was 7.62 mm long by 1.52 mm wide by 0.76 mm thick.

The TEM disks were irradiated in the JAERI triple ion facility (TIARA) using 12 MeV Ni ions with an irradiation rate of 1×10^{-3} dpa/s at a temperature of 200°C. The TRIM85 code [8] was used to compute the required ion fluences and the displacement dose as a function of depth beneath the specimen surface. The results of the TRIM calculation for the specified irradiation conditions are shown in Fig. 1. The solid line goes with the left axis and shows the damage in dpa as a function of depth in the specimen. The peak dose is about 30 dpa around 2 μm . The dashed line goes with the right axis and shows the injected Ni ions as a function of depth. The peak (0.7 at.%) occurs at about 2 μm . Both the displacement dose and Ni content in the ion irradiated TEM disk are varying as shown in Fig. 1. The

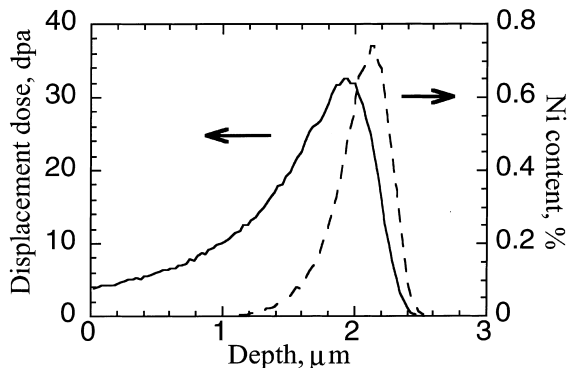


Fig. 1. Displacement dose and Ni ion content obtained from the TRIM calculation as a function of depth in the TEM disk irradiated with 12 MeV Ni ions. The solid and dashed lines correspond to displacement dose and Ni ion content, respectively.

effect of injected Ni ions on the microhardness of the TEM disk is neglected in this experiment because Ni is one of the main elements of the JPCA.

The tensile specimens were irradiated in the removable beryllium (RB^{*}) position of the High Flux Isotope Reactor (HFIR) to a dose level of 10 dpa and a helium level of 92 appm at a temperature of 200°C. The dose and helium levels were estimated from the reactor power data. A shield material surrounded the RB^{*} position capsule in order to reduce the thermal neutron flux and maintain a He/dpa level near that expected in a fusion reactor. The He/dpa ratios of the specimens were about 9. The detailed irradiation condition of the capsule was reported elsewhere [9]. After irradiation, some of the TEM and tensile specimens were annealed at 500°C for 8 h in a vacuum.

Microhardness tests were carried out on the surface of the TEM disk at room temperature. A microhardness testing machine, DUH-200 (Shimadzu Co.), was used for the hardness testing. A load was applied with a loading speed of 2.6×10^{-3} N/s, held 1 s and then removed. The load was continuously monitored along with the displacement with a resolution of 20 mN (2 mgf) and 0.01 μm , respectively. An Instron universal testing machine was used for the tensile testing. The specimens were tested at a temperature of 200°C with a strain rate of 1×10^{-3} s⁻¹ under vacuum. The 0.2% offset yield strength (YS) and ultimate tensile strength (UTS) were obtained from the engineering load–elongation curve of each specimen. The Eu determined by the conventional method was not adequate in the irradiated specimens because of a load drop just after yielding and a low work-hardening rate on the engineering load–elongation curve [3,4]. In the present work, a strain to necking (STN) [3] which is measured at a characteristic value of the stress decrease rate (5 MPa/%) as measured backwards from the end of the tensile curve was used in the results and discussion instead of Eu. A reduction of area (RA) of some specimens were calculated from the fracture surface area.

3. Results and discussion

The relationship between load and depth from the surface under loading in the microhardness test was given by $L/d = A + Bd$, where d is a depth (μm) from the surface, L is the load (N) at that depth, and A and B are

constants [10]. In particular, the value of B is in direct proportion to the microhardness of the material [11]. Fig. 2 shows load/depth–depth curves of SA and CW obtained from the microhardness tests. Both of the figures include the results of the unirradiated, the ion irradiated and the ion irradiated after annealing. The initial stage in each curve is neglected because this part of the curve includes a surface effect of the specimen. For SA, the slope of the unirradiated line, which corresponds to B in the equation, is about 3. The slope of the ion irradiated curve is about three times as high as that of the unirradiated curve up to a depth of 0.4 μm and then decreases to 3. It means that the microhardness of the ion irradiated is as low as that of the unirradiated over 0.4 μm depth. The ion injected layer (about 2 μm)

affects the microhardness of the ion irradiated up to 0.4 μm depth. This tendency was observed in another study using the same technique [12]. The slope of the ion irradiated specimen decreases to 4 up to 0.8 μm depth by annealing. It is considered that the change is attributed to thermal diffusion of defects induced by ion irradiation. A similar trend is induced in CW by post-irradiation annealing as shown in Fig. 2(b). The microhardness of both SA and CW increases after ion irradiation and then decreases after annealing. The results indicate that the hardening of the materials by ion irradiation is recovered by annealing.

The engineering stress–strain relationship of the irradiated SA and CW specimens was significantly influenced by annealing as shown in Fig. 3. The load drop just after

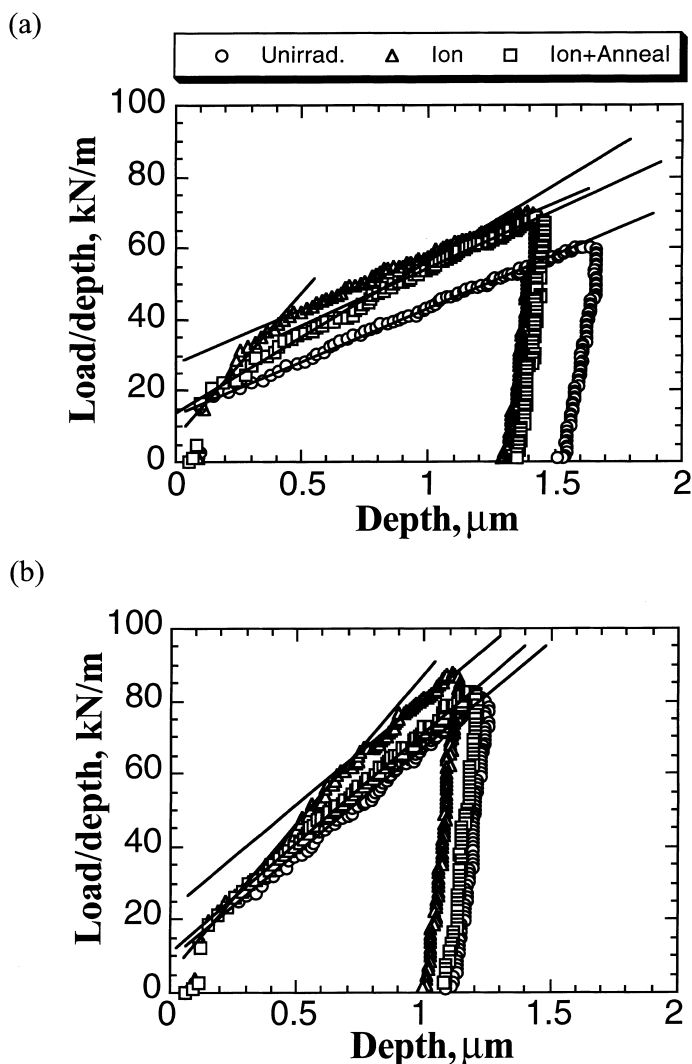


Fig. 2. A comparison of the relationship between $L(\text{load})/d(\text{depth})$ and d of (a) JPCA SA and (b) JPCA CW before and after annealing.

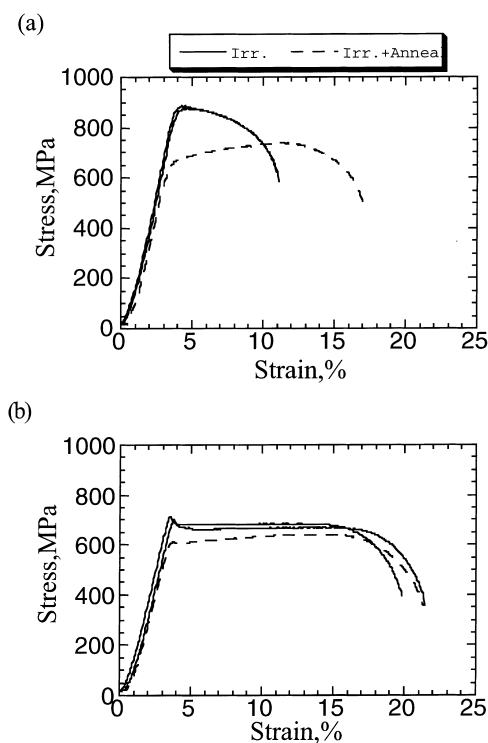


Fig. 3. Annealing effect on the engineering stress–strain relationship of (a) JPCA SA and (b) JPCA CW irradiated by neutron to a dose of 10 dpa at a temperature of 200°C.

yielding of the SA specimen disappears and the STN of the CW increases by annealing. Fig. 4 shows changes in YS, UTS, STN, Et and RA of the SA and CW by annealing. The data of SA and CW unirradiated specimens are obtained at a temperature of 250°C. For the irradiated SA, the YS and the UTS decrease to 610 and 640 MPa by annealing, respectively. Both of them are greater than those of the unirradiated. There is no significant increase of the STN, the Et, or the RA by annealing. The YS of the irradiated CW increases from 600 to 860 MPa by irradiation, and then decreases to 650 MPa by annealing. The change in UTS is similar to that in YS. The RA, even the STN and the Et, increases by annealing. The failure mode remains ductile in each case.

Several authors have related the strength of austenitic stainless steel to the microstructure produced during irradiation [13–15]. The defects that contribute to strength in the irradiated austenitic stainless steel have been divided into long range obstacles (network dislocations) and short range obstacles (black dots, stacking fault loops, precipitates and bubbles) [14]. The dislocation loops were induced in a Ni alloy by Ni ion irradiation at 425°C [16]. Small black dots with a very high density, but no cavities or precipitates, were observed in

austenitic stainless steel after neutron irradiation up to 250°C [17]. The defects induced by both ion and neutron irradiation at lower temperatures were mainly the dislocation loops. Moreover, the damaged microstructure, which consists of a very high density of tiny defects in type 304 stainless steel irradiated by neutron at a low temperature, was changed to a black dot and stacking fault loop structure (which can be treated together as small dislocation loops) by post-irradiation annealing (400°C, 1 h) [18]. The same authors also reported that helium bubbles were observed after high temperature annealing at 650°C for 1 h. Therefore, it seems that the change in the damaged microstructure of both ion and neutron irradiated specimens after annealing is an increase in diameter of dislocation loops and a decrease in density of dislocation loops. The change in yield strength of the neutron irradiated tensile specimens is similar to that in the microhardness of the ion irradiated TEM disks by annealing. Moreover, it is well known that a hardness can be related to a yield strength [19]. It is considered that the change in yield strength of the neutron irradiated tensile specimen by annealing can be predicted by the change in microhardness of the ion irradiated TEM disk.

4. Conclusions

The following conclusions can be drawn from this study.

1. The microhardness of both SA and CW materials increases after ion irradiation and then decreases by annealing.
2. The yield strengths of the irradiated SA and CW materials decreased after annealing by about 100 and 200 MPa, respectively. The strain to necking of the irradiated CW materials recovered from 0.7% to 7.6% after annealing.
3. The reduction of area of both SA and CW materials increase by annealing. The failure mode remains ductile in each case.
4. The change in yield strength of the neutron irradiated tensile specimen by post-neutron-irradiation annealing can be predicted by the change in hardness of the ion irradiated TEM disk.

Acknowledgements

The authors would like to thank Drs. A.F. Rowcliffe and M.L. Grossbeck for their cordial cooperation in the Japan–US collaborative testing. The authors also appreciate the help by Dr. E. Wakai. The tensile testing was performed by R.L. Martin and L.T. Gibson.

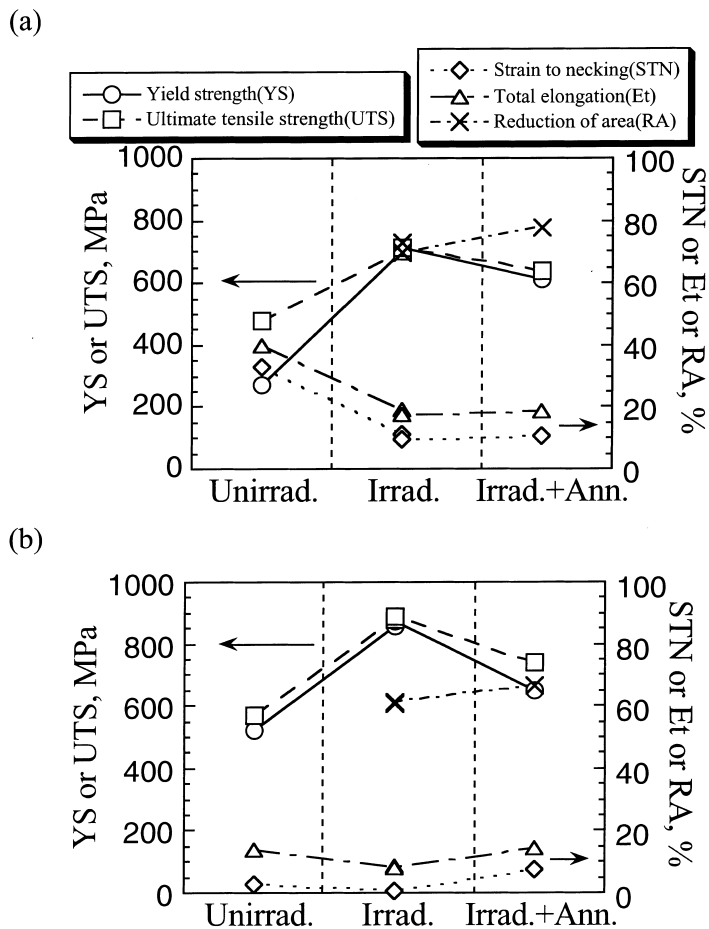


Fig. 4. A change in 0.2% yield stress, ultimate tensile strength, strain to necking and reduction of area of (a) JPCA SA and (b) JPCA CW specimens after post-irradiation annealing.

References

- [1] G.R. Odette, G.E. Lucas, *J. Nucl. Mater.* 179–181 (1991) 572.
- [2] S. Jitsukawa, M.L. Grossbeck, A. Hishinuma, *J. Nucl. Mater.* 191–194 (1992) 790.
- [3] M.G. Horsten, M.I. de Vries, in: *Effects of Radiation on Materials*, ASTM STP 1270, American Society for Testing and Materials, 1996, p. 919.
- [4] J.P.E. Robertson, I. Ioka, A.F. Rowcliffe, M.C. Grossbeck, S. Jitsukawa, in: *Effects of Radiation on Materials*, ASTM STP 1325, American Society for Testing and Materials, Boston (in press).
- [5] S. Majumdar, *Fusion Eng. and Design* 29 (1994) 158.
- [6] E.E. Bloom et al., *J. Nucl. Mater.* 22 (1967) 68.
- [7] A.J. Jacobs, G.P. Wozadlo, G.M. Gordon, *Corrosion* 52 (1995) 731.
- [8] J.F. Ziegler, J.P. Biersack, U. Littmark, *The Stopping and Range of Ion in Solids*, vol. 1, Pergamon, New York, 1985.
- [9] L.R. Greenwood, C.A. Baldwin, B.M. Oliver, *DOE/ER-0313/17* (1995) 28.
- [10] F. Froehlich, P. Grau, W. Grellmann, *Phys. Stat. Sol.* 42 (1977) 79.
- [11] H. Takahashi et al., *Development of Evaluation Techniques for Small Specimens*, Atomic Energy Society of Japan, 1992, p. 84.
- [12] Y. Katoh, T. Muroga, T. Iwai, O. Motojima, *J. Japan Inst. Metals* 61 (1997) 191.
- [13] R.L. Simons, L.A. Hulbert, in: *Effects of Radiation on Materials*, ASTM STP 870, American Society for Testing and Materials, 1985, p. 820.
- [14] M.C. Grossbeck, P.J. Maziasz, A.F. Rowcliffe, *J. Nucl. Mater.* 191–194 (1992) 808.
- [15] G.E. Lucas, *J. Nucl. Mater.* 206 (1993) 287.
- [16] D.H. Plantz, L.M. Wang, R.A. Dodd, G.L. Kulcinski, *Metall. Trans. A* 20 (1989) 2681.
- [17] S.J. Zinkle, P.J. Maziasz, R.E. Stooler, *J. Nucl. Mater.* 206 (1993) 266.
- [18] Y. Ishiyama, M. Kodama, N. Yokota, K. Asano, T. Kato, K. Fukuya, *J. Nucl. Mater.* 239 (1996) 90.
- [19] J.R. Cahoon, W.H. Broughton, A.R. Kutzak, *Metall. Trans.* 2 (1971) 1979.